

Surface lattice dynamics of nearly incommensurate overlayers

J. E. Black

Department of Physics, Brock University, Saint Catharines, Ontario, Canada L2S 3A1

D. L. Mills

D. L. Mills Department of Physics, University of California, Irvine, Irvine, California 92717

(Received 20 February 1990)

A monolayer adsorbed on a crystal surface may form an overlayer whose unit-cell dimension in one or both principal directions is very long compared with the substrate lattice constant (5–15 lattice constants, for example). We refer to such overlayers as nearly incommensurate. In this paper, we explore the lattice vibrations of such overlayers, within a model where the substrate is viewed as rigid, providing a corrugated potential well within which the adsorbates reside. We first find the static equilibrium configuration of the adlayer, and then calculate the phonon spectrum and mean-square displacements within harmonic lattice dynamics. For small corrugation amplitudes, we find very large mean-square displacements parallel to the surface. There is a smooth transition to a regime where the overlayer is locked to the substrate tightly; the transition occurs within a rather narrow range of corrugation strengths. This and other systematic aspects of the vibrational properties of such overlayers are explored in the paper.

I. INTRODUCTION

When an adsorbate overlayer is present on a crystal surface, a rich variety of structures is realized. The geometry of the overlayer, and its relation to that of the substrate, is controlled both by the nature of the bonding between the adsorbates and the substrate, and the strength of the adsorbate-adsorbate interactions.

One simple limit is that where there is strong chemical bonding between the adsorbate and substrate; the adsorbate is said to be chemisorbed. It will be found in a high-symmetry site, usually where the coordination number is highest. Examples would be the fourfold hollow site of the (100) surface of fcc crystal or the threefold hollow site of its (111) surface. At appropriate coverages one realizes commensurate overlayers, with islands of such structure at coverages in between those where commensurability is realized.

A very different limit applies to a closed-shell atom, such as a rare-gas atom adsorbed on a smooth metal surface. The adsorbate is "rigid" in its electronic structure to an excellent approximation and is bound to the substrate only by virtue of the rather weak van der Waals attraction. This is the case of physisorption. If the metal surface is very smooth, then at monolayer coverage the separation between adsorbates is controlled only by their mutual interactions. In this case, the monolayer is incommensurate with the substrate. An example of this behavior is provided by the overlayers of heavy-rare-gas atoms on the Ag(111) surface, which is very smooth.¹ On a more corrugated substrate, such as Pt(111), both incommensurate and commensurate rare-gas overlayers are found, as demonstrates by the elegant experiments of Kern and Cosma.²

The lattice dynamics of the two classes of overlayer just mentioned differ dramatically. Consider first the in-

commensurate monolayer, and assume that the x axis is parallel to a direction of incommensurability.³ Clearly, the energy of the system is left unchanged as one displaces the overlayer by an arbitrary amount ϵ parallel to the x axis. If one considers the surface phonons associated with such a substrate/adsorbate combination, then there must be a mode whose frequency vanishes as its wave vector Q_{\parallel} vanishes, when Q_{\parallel} is directed along the x axis. As $Q_{\parallel} \rightarrow 0$ in this manner, the polarization of the mode is parallel to the surface, and the eigenvector becomes entirely localized within the overlayer itself. This is a Goldstone mode of the adsorbate/substrate combination; its existence is guaranteed by the invariance of the energy of the overlayer/substrate combination to the translation just described.

For the incommensurate overlayer, we then have a "soft mode" whose frequency vanishes as Q_{\parallel} vanishes and the motion is localized within the layer in the limit. We may expect very large atomic mean-square displacements at finite temperature, parallel to the surface and to the x direction. If the overlayer is incommensurate as one moves parallel to x , but is commensurate along a second, noncolinear direction, the mean-square displacement will be finite, in the harmonic approximation of lattice dynamics. If the overlayer is incommensurate in both directions in the surface plane, then we have a phonon whose frequency vanishes as $Q_{\parallel} \rightarrow 0$ from *any* direction; in this limit, this mode again will be localized within the overlayer and polarized parallel to this surface. The presence of this mode leads to a divergence of the mean-square displacement in the harmonic approximation.

The commensurate overlayer behaves very differently. Any surface phonon whose amplitude is localized to the surface as $Q_{\parallel} \rightarrow 0$ will have finite frequency. The only surface mode with frequency that vanishes in this limit is the Rayleigh surface phonon, whose existence is

guaranteed and required by the theory of elasticity.⁴ As $Q_{\parallel} \rightarrow 0$, the Rayleigh wave penetrates deeply into the crystal, a distance the order of Q_{\parallel}^{-1} . One encounters no anomalous behavior in the mean-square displacement of the overlayer in this instance.

The purpose of this paper is to explore, within a model, aspects of the lattice dynamics of overlayers we have come to view as a third class. These are commensurate with the substrate, with a unit cell $N \times M$ in size, where either N or M or both may be integers large compared to unity. We refer to these as nearly incommensurate overlayers, and the analysis presented here suggests they may exhibit rather unusual behavior, as we discuss below.

An example of such an adsorbed overlayer is a Ag monolayer on Ni(100), which forms a (2×8) structure.⁵ The Ag overlayer is distorted only very slightly ($\sim 1\%$) from the hexagonal atomic layer one finds as a (111) plane in the bulk Ag crystal. Evidently, the Ag-Ag spacing is such that the overlayer requires only a very small distortion to lock into the underlying (square) lattice one finds on the Ni(100) surface. If one moves along the direction in the unit cell which contains eight Ni atoms, there are seven Ag atoms within this length. The Ag overlayer on Cu(100) forms a (2×10) structure.⁵

In an earlier paper,⁵ we developed an approximate but accurate description of the surface lattice dynamics of such structures, which contain a large number of atoms per unit cell and thus are difficult to analyze with standard methods. This was done with a force constant model, which did not take account of the detailed structure of the overlayer; i.e., all adsorbates were assumed to lie in a plane a given distance above the substrate, and no relaxation parallel to the surface was incorporated. Thus we confined our attention to a flat, ideal, 2×8 overlayer coupled to nearby substrate atoms with appropriate "springs." In the end, with a simple model of the force constant, we obtained an excellent account of off-specular electron scattering studies of the Rayleigh surface phonon of the structure.⁵ We did not explore the character of atomic motions parallel to the surface.

In this paper, within the framework of a model, we wish to study lattice vibrations of nearly incommensurate overlayers, with attention to the role of relaxation and the character of atomic motions parallel to the surface. Our motivation is the following.

We may expect parallel mean-square displacements in a truly incommensurate overlayer to be large, for the reasons mentioned above. The question is, for the case of high-order commensurability, with N rather large (say, in the range of 5–10), does one realize very large parallel mean-square displacements, as expected for an incommensurate overlayer, or is the Goldstone mode suppressed by locking of the overlayer to the substrate, to the point where the parallel mean-square displacement is rather ordinary in magnitude? We find, for the model examined here, that the "lock-in" energy is in fact remarkably small, for the reasons described below. This result is obtained for modest corrugations. There is thus rather little difference, so far as the phonon spectrum is concerned, between the truly incommensurate overlayer and one which exhibits high-order commensurability.

The model is one in which the substrate is viewed as quite rigid, with a profile that is corrugated. A given adatom then feels a potential from the substrate we write as $V(\mathbf{r}_{\parallel}, z)$, where its position is $\mathbf{r} = \mathbf{r}_{\parallel} + z\hat{\mathbf{z}}$, with z normal to the surface plane and \mathbf{r}_{\parallel} the projection of \mathbf{r} onto it. The form for $V(\mathbf{r}_{\parallel}, z)$ we use is discussed below.

We then bring down a monolayer of adatoms onto the rigid, corrugated potential. These interact by means of nearest-neighbor couplings of the form $\frac{1}{2}k(r_{nm} - r_0)^2$, where r_0 , an input parameter, is the free-space equilibrium spacing between adatoms. Our interest is in the case where the value of r_0 is such that the adlayer placed in free space is very nearly commensurate with the substrate, where a small distortion will lead to an $N \times M$ structure, with N or M large. We allow the atoms to relax to equilibrium positions, by moving both vertically and horizontally. When the adlayer "locks in" to the substrate, we have a relaxation energy ΔE we may call the lock-in energy. Once the equilibrium structure is found, we then explore the spectrum of surface phonons associated with the structure and calculate the mean-square displacements within the framework of harmonic lattice dynamics. As remarked earlier, our principal conclusion is that the lock-in energy is remarkably small for modest corrugations. When N or M is large, the cost in energy to slide the line parallel to the surface is very small; a consequence is that the mean-square displacement we calculate (in the harmonic approximation) is very large.

In Sec. II, we introduce the model that forms the basis for our analysis, and we can appreciate by means of a simple discussion the reason why ΔE is so small. Section III presents our full numerical analysis, and Sec. IV explores the implications of the results.

II. INTRODUCTION OF THE MODEL AND GENERAL COMMENTS

For the adatom-substrate potential, we use a form

$$V(\mathbf{r}_{\parallel}, z) = V_0(z) + \sum_{\mathbf{G}_{\parallel} (\neq 0)} \Delta V(\mathbf{G}_{\parallel}) \exp(i\mathbf{G}_{\parallel} \cdot \mathbf{r}_{\parallel}) \times \exp(-G_{\parallel} z). \quad (2.1)$$

The first term, $V_0(z)$ contains an attractive van der Waals tail in principle ($\sim 1/z^3$) and a repulsive part at short range. It describes, phenomenologically, the physisorption well associated with a very smooth surface. The remaining terms provide the corrugation. If this piece of the potential has its origin in the distribution of static charge in the substrate, then at large values of z which lie outside the physical charge distribution, the potential must satisfy Laplace's equation. This dictates the z dependence displayed in the second terms of Eq. (2.1), at least for large z . We shall use this form for all values of z ; for our purposes, however, only the near vicinity of the minimum in the physisorption well is important. We assume the minimum in $V_0(z)$ lies at $z=0$ and suppose this is far enough from the outermost layer of nuclei for the z dependence of the corrugation terms to be reasonable. A surface that can be viewed as exhibiting a sinusoidal cor-

rugation is described by retaining the set of terms in Eq. (2.1) associated with the star of reciprocal lattice vectors of shortest length. We then just have one nonzero parameter, since symmetry may be used to interrelate the various coefficients associated with this star, all of which must have the same magnitude.

Once again, the adatom-adatom interactions are introduced by assuming these are of nearest-neighbor character and given by $\frac{1}{2}k(r_{nm}-r_0)^2$, where k and r_0 are parameters, and r_{nm} is the separation between atoms n and m .

It is instructive to examine first a one-dimensional model of the structures explored below. Let us consider a row of adatoms arranged along the x axis; vertical relaxation or motions will be ignored. The potential energy of the array is then

$$U = \frac{1}{2}\Delta V_1 \sum_n \cos\left(\frac{2\pi}{a_0}x_n\right) + \frac{1}{2}k \sum_n (x_{n+1} - x_n - x_0)^2. \quad (2.2)$$

This model has been explored extensively in the theoretical literature.⁶ We examine some features of it here, with attention to the questions that motivate our study.

The equilibrium condition is found from $\partial u / \partial x_n = 0$ for all x_n . If we write $x_n = a_0 y_n$, then to find the equilibrium positions, we must solve

$$y_{n+1} + y_{n-1} - 2y_n + \alpha \sin(2\pi y_n) = 0, \quad (2.3)$$

where $\alpha = \pi \Delta V_1 / ka_0^2$. If we also let $x_0 = a_0 y_0$, then the potential energy of the array is

$$U = \frac{1}{2}ka_0^2(E_s + E_e), \quad (2.4)$$

where

$$E_s = \frac{\alpha}{\pi} \sum_n \cos(2\pi y_n) \quad (2.5)$$

is the interaction energy of the adatoms with the substrate, and

$$E_e = \sum_n (y_{n+1} - y_n - y_0)^2 \quad (2.6)$$

is the elastic energy stored in the array.

When $\alpha=0$ (a trivial limit, of course), we then have a set of adatoms that are spaced uniformly, with separation $\Delta y=1$ (or $\Delta x=x_0$). We shall make a special choice of y_0 , $y_0=M/N$, where M and N are both integers. One can show that this value of y_0 corresponds to a local minimum in the energy of system. With this choice, in a piece of substrate whose real-space length is Ma_0 , we have N adatoms. The choice $N=7$ and $M=8$ allows one to mimic Ag on Ni(100), in the limit the Ni surface is viewed as perfectly smooth.

When $\alpha=0$, we denote the position of mass n by $y_n^{(0)}$. We write

$$y_n^{(0)} = \Delta + ny_0, \quad (2.7)$$

where Δ is a position of a fiducial mark on the line of atoms. A change in Δ slides the line along the x axis.

Now suppose the surface is weakly corrugated, a limit that applies to low index surfaces of metals (we comment further on this below). We may expand the energy in powers of the corrugation parameter α . It will be useful to explore the structure of this expansion.

To begin, we expand the displacement in powers of α , thus allowing the masses to relax:

$$y_n = y_n^{(0)} + \epsilon_n^{(1)} + \epsilon_n^{(2)} + \dots, \quad (2.8)$$

where $\epsilon_n^{(1)}$ and $\epsilon_n^{(2)}$ are, respectively, first and second order in α . From the equilibrium condition [Eq. (2.3)], we find

$$\epsilon_n^{(1)} = \frac{\alpha}{4} \frac{\sin(2\pi y_n^{(0)})}{\sin^2(\pi y_0)}, \quad (2.9)$$

and

$$\epsilon_n^{(2)} = \frac{\pi\alpha^2}{16} \frac{\sin(4\pi y_n^{(0)})}{\sin^2(\pi y_0)\sin^2(2\pi y_0)}. \quad (2.10)$$

For the moment, we regard y_0 as an irrational number very close to M/N in value; as we examine various terms in the perturbation expansion, we shall take the limit $y_0 \rightarrow M/N$.

The energies E_s and E_e may also be expanded. If we keep terms through those cubic in α , then in a unit cell that contains N adatoms, the energy per atom is

$$\begin{aligned} \frac{E_s}{N} &= \frac{\alpha}{\pi N} \sum_{n=0}^{N-1} \cos(2\pi y_n^{(0)}) - \frac{2\alpha}{N} \sum_{n=0}^{N-1} \sin(2\pi y_n^{(0)}) \epsilon_n^{(1)} \\ &\quad - \frac{2\alpha}{N} \sum_{n=0}^{N-1} [\cos(2\pi y_n^{(0)}) \epsilon_n^{(1)2} \\ &\quad \quad \quad + \sin(2\pi y_n^{(0)}) \epsilon_n^{(2)}] + \dots \end{aligned} \quad (2.11)$$

and

$$\begin{aligned} \frac{E_e}{N} &= \frac{1}{N} \sum_{n=0}^{N-1} (\epsilon_{n+1}^{(1)} - \epsilon_n^{(1)})^2 \\ &\quad + \frac{2}{N} \sum_{n=0}^{N-1} (\epsilon_{n+1}^{(1)} - \epsilon_n^{(1)}) (\epsilon_{n+1}^{(2)} - \epsilon_n^{(2)}) + \dots \end{aligned} \quad (2.12)$$

To first order in α , we evaluate the leading term in Eq. (2.11), which describes the interaction of a rigid, unrelaxed row of adatoms with the corrugated substrate:

$$\frac{E_s^{(1)}}{N} = \frac{E_s^{(1)}}{N} = \frac{\alpha}{\pi N} \sum_{n=0}^{N-1} \cos(2\pi y_n^{(0)}), \quad (2.13)$$

or upon performing the sums,

$$\frac{E_s^{(1)}}{N} = \frac{\alpha}{\pi N} \frac{\sin(\pi N y_0)}{\sin(\pi y_0)} \cos\{\pi[2\Delta + (N-1)y_0]\}. \quad (2.14)$$

While there is a periodic dependence on Δ in Eq. (2.14), and thus we have a contribution to the ‘‘lock-in’’ energy first order in α , as $y_0 \rightarrow M/N$ the numerator vanishes identically, *unless* M/N is an integer. In the latter case, the numerator and denominator vanish simultaneously, and

$$\frac{E_s^{(1)}}{N} \rightarrow \frac{\alpha}{\pi} \cos\{\pi[2\Delta + (N-1)y_0]\}. \quad (2.15)$$

If, as in our example with $M=8$ and $N=7$, M/N is not an integer, then we must look to the terms second order in α to find a contribution to the lock-in energy.

Note that this means that the lock-in energy has its physical origin in the substrate-induced relaxation of the structure.

It is straightforward, though a bit tedious, to work out the second-order terms. One finds, assuming y_0 is not an integer,

$$\frac{E_s^{(2)}}{N} = -\frac{\alpha^2}{4 \sin^2(\pi y_0)} \left[1 - \frac{1}{N} \frac{\sin(2\pi N y_0)}{\sin(2\pi y_0)} \cos\{2\pi[2\Delta + \pi(N-1)y_0]\} \right] \quad (2.16a)$$

and

$$\frac{E_e^{(2)}}{N} = \frac{\alpha^2}{8 \sin^2(\pi y_0)} \left[1 + \frac{1}{N} \frac{\sin(2\pi N y_0)}{\sin(2\pi y_0)} \right]. \quad (2.16b)$$

The dependence on Δ resides in the second term in Eq. (2.16a). For the coefficient of this term to be nonzero, we require both $\sin(2\pi N y_0)$ and $\sin(2\pi y_0)$ to vanish as $y_0 \rightarrow M/N$. This means the ratio $2M/N$ must be an integer. When this is the case, we obtain a contribution to the lock-in energy of order α^2 .

To make the trend clear, we assume $2M/N$ is not an integer, and we examine the terms cubic in α . These yield

$$\frac{E_s^{(3)}}{N} = \frac{\alpha^3}{32 \sin^4(\pi y_0)} \frac{1}{N} \left[1 + \frac{2\pi \sin^2(\pi y_0)}{\sin^2(2\pi y_0)} \right] \left[\frac{\sin(3\pi N y_0)}{\sin(3\pi y_0)} \cos\{3\pi[2\Delta + (N-1)y_0]\} - \frac{\sin(\pi N y_0)}{\sin(\pi y_0)} \cos\{\pi[2\Delta + (N-1)y_0]\} \right] \quad (2.17a)$$

and

$$\frac{E_e^{(3)}}{N} = \frac{\alpha^3}{16 \sin^3(\pi y_0) \sin(2\pi y_0)} \frac{1}{N} \left[\frac{\sin(3\pi N y_0)}{\sin(3\pi y_0)} \cos[3\pi(N y_0 + 2\Delta)] + \frac{\sin(\pi N y_0)}{\sin(\pi y_0)} \cos[\pi(N y_0 + 2\Delta)] \right]. \quad (2.17b)$$

In this order, we now obtain a contribution to the lock-in energy if $3M/N$ is an integer.

The criterion for locating the first nonzero contribution to the energy which contains a dependence on Δ is now quite clear. The first contribution will be the order of α^s , where s is the smallest integer which makes sM/N an integer. In our representation of Ag on Ni(100), where we would choose $M=8$ and $N=7$, the lowest order contribution will be the term proportional to α^7 ! When $\alpha < 1$, this means the lock-in energy is very small indeed. There is very little difference between the truly incommensurate overlayer and the nearly incommensurate structure, at least for weakly corrugated surfaces with $\alpha \ll 1$.

The discussion above assumes the nature of the adatom-adatom interaction is such that $y_0 = M/N$, where M and N are integers presumably in the range of 1–10, and so we can speak of a unit cell of the adsorbate/substrate complex whose length contains a few substrate atoms. Of course, it is unlikely that in a real physical system the equivalent of y_0 assumes such a special value. However, the properties of systems studied to date suggest that y_0 can lie very close to such a value. The Ag overlayer on Ni(100), which we have remarked forms a (2×8) structure, is distorted from a bulk Ag(111) crystal plane by an amount the order of 1%, in each of the two directions in the surface plane. Such a small distortion of the bulk Ag(111) plane generates an overlayer

that comes into precise registry with the Ni(100) substrate, as a (2×8) adlayer. This suggests that we can model a line of Ag atoms parallel to the direction where the repeat distance is eight substrate atoms by choosing $y_0 = \frac{8}{7} + \eta$, where η is very small in magnitude, the order of 0.01. A very small adjustment of the mean spacing between adatoms will then allow the line to “lock in” to the substrate.

To obtain a description of the lock-in energy in this situation, when the surface is weakly corrugated, we should extend the discussion given above, to generate a power series expansion for the energy of the structure in both α and η . We will not do this here; it is clear the lock-in energy will remain very small. For example, if the mean spacing between atoms changes by the amount η , the change in elastic energy per atom in the line of adsorbates is given by $\frac{1}{2}k\eta^2$, which is roughly $\frac{1}{2}\hbar\omega_M\eta^2$, where ω_M is the maximum phonon frequency of the line of adatoms. This is the first term in an expansion of the energy in powers of η and is, in fact, independent of Δ . It is also very small in magnitude. Contributions to the lock-in energy will appear in higher order. Thus, if we were to expand the energy in a power series in both α and η , it would remain the case that the contribution to the lock-in energy will be small.

The numerical calculations presented in the next section show that, for the systems considered, the lock-in energy is remarkably small, until the corrugation strength

becomes substantial. Indeed, it proved challenging to calculate it accurately in the parameter range of interest. The purpose of the discussion in this section was to understand why this energy is so small. This is the origin of the very large parallel mean-square displacements we have calculated; nearly incommensurate structures on weakly corrugated surfaces are remarkably "soft," with respect to long-wavelength atomic motions parallel to the surface.

III. QUANTITATIVE STUDIES OF THE MODEL: RELAXATION OF THE STRUCTURE, THE PHONON SPECTRUM, AND THE MEAN-SQUARE DISPLACEMENT

Since this study is motivated by earlier experimental and theoretical analyses of the Ag monolayer on Ni(100), we depict this structure and its Brillouin zone in Fig. 1. We construct a representation of this overlayer by placing one Ag atom in the fourfold hollow site, at the origin of the coordinate system. Then, in the y direction, we place seven Ag atoms (equally spaced in the figure, in which relaxation is ignored) over a distance parallel to y that contains eight substrate atoms. The second line of

Ag atoms is constructed parallel to the first, with each atom halfway between two lines of Ag atoms constructed as just described. As noted in Ref. 5, the Ag overlayer constructed in this manner is only very slightly distorted from the Ag(111) plane of elemental silver; the distortions are the order of 1%. The primitive unit cell of the structure is the 1×8 form indicated in the figure.

We wish to begin with such a structure with adsorbates equally spaced and allow the atoms to relax both in the vertical direction and in the plane of the surface. The relaxation is in response to the substrate potential in Eq. (2.1). If $\Delta u(I)$ is the displacement of the atom at site I , then clearly from symmetry considerations, $\Delta u(I)$ lies in the yz plane. Thus, for purposes of analyzing relaxation of the adlayer, we may represent the substrate as a one-dimensionally corrugated grating, with peaks and valleys

$$V(\mathbf{r}_{\parallel}, z) = V_0(z) + \Delta V \exp(-Gz)[1 - \cos(Gy)], \quad (3.1)$$

where $G = 2\pi/a_0$, with a_0 the substrate lattice constant. For $V_0(z)$, we use the Morse form

$$V_0(z) = V_0[\exp(-2\sigma z) - 2\exp(-\sigma z)]. \quad (3.2)$$

The minimum of $V(z)$ is at $z=0$, where we have an adsorption well of depth V_0 . Here we are primarily concerned with the behavior of $V_0(z)$ in the vicinity of $z=0$, and so we need not be concerned about a complete description of it, including the van der Waals tail.

Interactions between the nearest neighbors in the adatom overlayer will have the form

$$V_{\text{int}} = \frac{1}{2} k \sum_{ij} (|\mathbf{r}_i - \mathbf{r}_j|^2 - r_0^2)^2, \quad (3.3)$$

where the sum is over nearest-neighbor pairs. We shall be choosing parameters so our results provide a description of the Ag overlayer on Ni(100). We choose $k = 2.02 \times 10^4$ dyn/cm, a value that provides a reasonable representation of bulk Ag phonons, as discussed in the paper by Black, Shanes, and Wallis.⁷ We choose r_0 to be the nearest-neighbor distance in Ag; so $r_0 = 2.89$ Å.

We shall be employing reduced units of length and frequency, as we present our results. Lengths will be measured in units of the bulk nearest-neighbor distance of Ni, which is 2.49 Å. In reduced units, $r_0 = 1.1619$. Frequencies will be measured in units of $(k/M_{r=\text{Ag}})^{1/2}$, which equals 56.4 cm^{-1} .

We have three more parameters, V_0 , σ , and ΔV . We determine them via the following constraints.

(a) The fourfold hollow site lies on the line $y=0$, and the bridge site at $y=a_0/2$. We assume that the distance between an isolated Ag atom in the fourfold hollow and its four nearest-neighbor Ni atoms will be 2.59 Å, the average of the Ag-Ag and the Ni-Ni distances in the bulk. We assume that an isolated Ag atom in the bridge site is also separated from its two nearest Ni neighbors by 2.59 Å. This places the bridge site 0.35 Å above the hollow site, and we require this to be the case.

(b) The data reported in Ref. 5 suggest the average Ag perpendicular vibration frequency (with substrate held fixed) to be roughly 74 cm^{-1} [(1.3) reduced units]. Furthermore, the surface is rather smooth, and there seems lit-

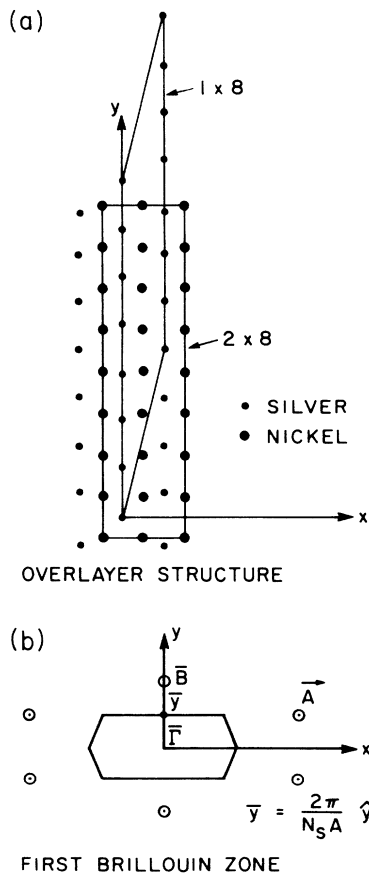


FIG. 1. The structure of the Ag overlayer on Ni(100), with relaxation neglected. (a) We show both the 2×8 unit cell of the substrate and also the 1×8 . (b) The reciprocal lattice corresponding to the 1×8 real-space unit cell. We show also the first Brillouin zone.

the evidence for a site dependence in the perpendicular vibration frequency. Thus we require the perpendicular vibration frequency for an isolated Ag adatom in both the fourfold hollow and the twofold bridge to be 74 cm^{-1} .

These constraints require $V_0 = 1.7 \text{ eV}$, and in reduced units $\sigma = 2.0$. Both values seem quite reasonable. We use as a measure of surface corrugation $\alpha = V_c \pi / ka_0^2$, where V_c is the energy difference between the equilibrium fourfold hollow and the equilibrium bridge site. Note that V_c is not equal to $2\Delta V$, in the presence of corrugation. From the constraints we find $\alpha = 0.12$, and so the substrate is inferred to be rather smooth. The discussion of Sec. II, which assumes α is small, is thus applicable. The energy difference between the hollow and bridge sites is 0.3 eV in this picture.

The above numbers are surely reasonable for the discussion of a metal adlayer on a metal substrate. We shall explore how our predictions are affected by variation of the above parameters, but these choices provide us with an initial starting point.

We now proceed as follows. We begin by placing an atom in a hollow site, as described earlier, and then arrange the adatoms in a perfect, two-dimensional lattice with the 1×8 primitive unit cell illustrated in Fig. 1. Initially, the spacing between adatoms is uniform, and all lie in the same plane parallel to the average surface. In this configuration, which is not an equilibrium configuration, there is a force on each atom from the substrate except for the atom in the hollow site. This force is determined, and each atom is displaced in a direction parallel to the force, and in an amount proportional to it. Each such move lowers the energy of the system. The process was repeated, until each force was below 10^{-9} in reduced units; initial forces were larger by roughly six orders of magnitude. In the end, we obtain the energy per atom, accurate to one part in 10^8 .

For $\alpha = 0.12$, we show the atomic positions in the equilibrium configuration (no forces) in Table I. We give three sets of information. On the left, we have the relaxed positions of a one-dimensional line of atoms, such as that considered in Sec. II. Then we have the two-dimensional adlayer, with one atom confined to the hollow site, and we also give relaxed positions for a second structure, where we begin by placing the initial atom on a bridge site. We can see that in both cases the two-

dimensional layer becomes rumpied, and that the displacements away from the starting position are smaller for the two-dimensional case, when compared to the one-dimensional line.

Each of the two structures summarized in Table I is in equilibrium, in the sense that no atom experiences a net force from the neighbors, to which it is coupled, and the substrate. It is not clear, however, that each corresponds to a (local) minimum in the potential energy. We may test this by calculating the frequencies of the various phonons.

When we do this, for the parameters above, for the array with one atom in the fourfold hollow site, the square of the frequency of the lowest frequency phonon of zero wave vector is negative. The frequency itself is thus pure imaginary. This is then an unstable equilibrium position. For the array with one atom in bridge site, the lowest frequency is 0.015692 in reduced units, which is very small in reduced units compared to 1.31 , the perpendicular vibration frequency of the isolated Ag atom. The argument presented in Sec. II suggests that this gap frequency should be the order of a typical vibration frequency, reduced by $\alpha^{3.5}$, and a numerical prefactor that can be generated only from a detailed analysis. This follows by noting the square of the gap frequency should be related to the curvature of the "lock-in" energy, divided by the atomic mass. One sees that $1.31\alpha^{3.5}$ lies within a fraction of the gap frequency just quoted. We comment on the variation with α below. For the unstable hollow site configuration, the square of the gap frequency is $-(0.015692)^2$ to high accuracy, suggesting that for the relaxed structure, the lowest term in α dominates the lock-in energy.

The difference in energy per atom of the two structure is very small; for the hollow site geometry, the energy per atom is 1.99709×10^{-2} reduced units, while for the bridge site, it is 1.99706×10^{-2} . The difference is 3×10^{-7} reduced units, quite close to $\alpha^7 (3.6 \times 10^{-7})$, as suggested in Sec. II. Clearly, the overlayer can be translated parallel to the surface with very little cost in energy.

We may also examine the one-dimensional line with $N = 7$ and $M = 8$, for a parameter set identical to that used for the two-dimensional simulation just described. The two-dimensional structure is much "softer," in the

TABLE I. Relaxed atom positions for $\alpha = 0.12$.

Atom number	One-dimensional case y_i	Initial atom in hollow site			Initial atom in bridge site		
		Initial positions y_i	Relaxation Δy_i	Δz_i	Initial positions y_i	Relaxation Δy_i	Δz_i
1	0.0000	0.0000	0.0000	0.0007	0.5000	0.0000	0.1437
2	1.0567	1.1428	-0.0394	0.0194	1.6428	+0.0342	+0.1127
3	2.1553	2.2857	-0.0451	0.0794	2.7857	+0.0476	+0.0453
4	3.3532	3.4286	-0.0182	0.1356	3.9486	+0.0021	+0.0050
5	4.6468	4.5714	+0.0182	0.1356	5.0714	-0.0021	+0.0050
6	5.8447	5.7143	+0.0451	0.0794	6.2143	-0.0477	+0.0453
7	6.9433	6.8571	+0.0394	0.0194	7.3571	-0.0342	+0.1127
9	8.0000	8.0000	0.0000	0.0007	8.5000	0.0000	0.1437

sense that the minimum phonon frequency in one dimension is 0.1302.

It is of interest to explore the variation in the magnitude of the gap, as various system parameters are varied. For example, we need not suppose the vibration frequency of an adatom in the fourfold hollow site is identical to that when it is adsorbed on the bridge site. If ν_B and ν_H are the bridge and hollow site frequencies, we may vary these holding the Ag-Ni distances identical to those described above. When this is done, for $\nu_B/\nu_H=0.8$ (this requires $\alpha=0.15$ and $\sigma=0.8$), we find the gap frequency to be 1.17×10^{-2} dimensionless units, smaller than 1.57×10^{-2} , corresponding to $\nu_B/\nu_H=1$. Similarly, the choice $\nu_B/\nu_H=1.2$ leads to a gap frequency of 1.80×10^{-2} . Variation of ν_B/ν_H affects the value of the gap frequency, but not its order of magnitude.

In Table II we show for $\alpha=0.12$ the variation of the energy per atom and the gap frequency with the parameter r_0 , which enters our model adsorbate-adsorbate interaction. It will be recalled that the equilibrium distance between adsorbates in a layer fully isolated from the substrate is r_0 . If the adlayer matches onto the substrate perfectly, to form a primitive unit cell which contains eight substrate atoms and seven adsorbate atoms, then in our reduced units one must have $r_0 = \frac{8}{7}$. Clearly, as expected, the energy/atom of the relaxed overlayer (bridge site geometry, which is the stable configuration) has a minimum at $x_0 = \frac{8}{7} = 1.1429$. However, for the parameters explored, the gap frequency increases monotonically with r_0 . In the limit of zero corrugation, with the rows of Ag arranged with the separation shown in Fig. 1, the structure of minimum energy is a slightly distorted hexagon with $x_0 = 1.1488$.

The effect of increasing corrugation is quite dramatic. We have varied the corrugation strength parameter α , with the isolated adsorbate frequency on both bridge and hollow sites held fixed and equal. This may be accomplished through appropriate choice of σ in the physisorption potential, and by doubling then tripling the original corrugation amplitude of 0.35 Å. The results are in Table III. This table shows results similar to those we have found in several studies. For rather small values of α , say, $\alpha \lesssim 0.10$, the gap in the phonon spectrum is really very small, and the gap varies dramatically with α , as expected from the arguments of Sec. II. We see in Table III that as α is increased by a factor of 2, from 0.12 to 0.24, the gap frequency increases by a factor of 10.2, not far

TABLE II. The energy per atom and gap frequency as a function of x_0 .

x_0	Energy/atom (10^{-2} reduced units)	Gap frequency (10^{-2} reduced units)
1.10	2.36	0.78
1.12	2.12	0.98
1.14	2.00	1.23
1.16	1.99	1.57
1.18	2.11	2.03
1.20	2.33	2.64

TABLE III. Effect of corrugation strength α on the energy per atom and the gap frequency at the zone center.

α	σ (reduced units)	Energy/atom (10^{-2} reduced units)	Gap frequency (reduced units)
0.12	2.0	1.997	0.0157
0.24	1.9	4.058	0.1605
0.36	1.7	6.082	0.3362

from the ratio expected (11.3) if the gap varied as $\alpha^{3.5}$, as suggested for the case from the arguments in Sec. II. As soon as the gap becomes an appreciable fraction of the maximum frequency 1.31, its variation with α becomes far more modest.

We show two additional illustrations of this behavior. In Table IV we see that doubling α from 0.06 to 0.12 again leads to an increase in the gap frequency that is a bit more than a factor of 10, while increasing α by 25% from 0.48 to 0.60 leads only to a 33% increase in the gap frequency. It should be remarked that for the calculations in Table IV we have chosen parameters so that isolated adatom frequency in the hollow and bridge sites are equal, and also so that the equilibrium height of the two sites are the same (that is, the corrugation is removed). In Fig. 2 we show the variation of the gap frequency with α for the one-dimensional line, with seven adsorbate atoms within a substrate unit cell that contains eight adatoms. For large α , the numerical results are fitted accurately by $\omega_0 = 3.305(\alpha - \alpha_c)$ where, as noted on the figure, $\alpha_c = 0.0755$. For the smallest α explored, say $\alpha \lesssim 0.06$ in this case, ω_0 scales as roughly $\alpha^{3.3}$, close to the $\alpha^{3.5}$ behavior expected from the arguments in Sec. II.

These results suggest the following picture of the nature of the relaxed adlayer. For small or rather modest

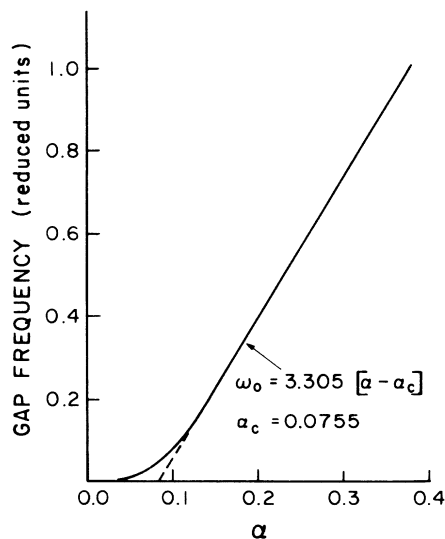


FIG. 2. For a one-dimensional system, in which the basic unit cell contains eight substrate repeat distances and seven adsorbate atoms, we show the variation of the gap frequency with α .

TABLE IV. Influence of corrugation parameter α on gap frequency. (These calculations are carried out for the case where the isolated adatom "sits" an equal distance above the surface in both the hollow and bridge sites; the perpendicular vibration frequency for the isolated adatom is also the same for both sites.)

α	Gap frequency (reduced units)
0.00	0.000
0.06	0.0022
0.12	0.0227
0.24	0.1980
0.36	0.5268
0.48	0.8680
0.60	1.1671

values of α , say, $\alpha \lesssim 0.10$ – 0.15 , the gap in the phonon spectrum is very small, and one may translate the adlayer across the substrate at a very small cost in energy per atom. The mean-square displacements parallel to the surface will be very large in this regime, as a consequence of the very small gap. We shall present calculations of the mean-square displacement in this regime below. As α increases, suddenly the gap increases rather dramatically with α , and by the time $\alpha \sim 0.3$ or larger, the gap in the phonon spectrum is a substantial fraction of the maximum phonon frequency of the substrate. In this regime, the adlayer is locked rather tightly to the substrate, and the parallel mean-square displacement is not anomalous. As one sees from Fig. 2, one passes from one regime to the other in a continuous manner. In our analysis, which is equivalent to a mean-field description of the system, there is no evidence of a phase transition. But there is a clear, continuous crossover between two distinct regimes.

It is interesting that our parametrization of the Ag overlayer on Ni(100) gives $\alpha \cong 0.12$, near the crossover region. It is reasonable to expect some metal overlayers on metal substrates may be described by values of α smaller than these by factors of 3 or 4. These would display large amplitude mean-square displacements parallel to the surface. On the other hand, a system with α larger by a factor of roughly 2 would lock in rather tightly to the substrate and display no anomalous behavior in this regard.

In Table V we present a study of the variation of the energy per atom and the gap frequency, with the number of adatoms per unit cell. These calculations are carried out for our simulation of the Ag overlayer on Ni(100). That is, we assume that the vibration frequency of an isolated atom in the hollow site is the same as that of such an atom in the bridge site; r_0 is chosen such that the isolated adlayer has spacing between neighbors equal to that found in a (111) plane of bulk Ag. This, combined with our model of the Ag—Ni bond length, leads to a height difference of 0.35 \AA between the hollow and bridge site, for reasons discussed earlier.

We give numbers for the two configurations discussed earlier in which there is zero force on each adatom in the array. One has an adatom localized in a hollow site and one adatom localized on a bridge site. The energy per atom for each configuration is remarkably close, in all cases. Considerable care was taken in these computations, and all figures displayed are significant. It is intriguing that the energy per atom is a minimum when there are seven adsorbates per unit cell, as realized in practice for the Ag adlayer on Ni(100).

We have seen earlier that for $N=7$ the bridge site configuration is a stable equilibrium configuration, in the sense that all phonon frequencies are real, while the bridge site is unstable. We see that as N increases, the most stable structure alternates, with the hollow site stable for $N=5, 9$, and 13 , and the bridge site for $N=7, 11$, and 15 .

So far, our examination of the lattice dynamics of the adsorbate array has focused only on the gap in the phonon spectrum which, as we have seen can be very small, and exhibits a strong variation with amplitude of the corrugation, as described by the parameter α . We have done this because in our two-dimensional model, the mean-square displacement parallel to the surface is influenced very importantly by the gap. We now turn our attention to the phonon spectrum of the nearly incommensurate overlayer and then to the mean-square displacement.

For the one-dimensional line, in Fig. 3 we show the phonon spectrum for two cases, $\alpha=0.05$ and 0.40 . Dimensionless units of both frequency and wave vector are used. The Brillouin zone is appropriate to a structure with seven atoms per unit cell, and so each panel contains seven phonon branches. Note the very small gap at $q=0$ for the lowest branch, for the case $\alpha=0.05$, while for

TABLE V. Energy per adatom and gap frequency as a function of the number of adatoms per unit cell.

No. of adatoms per unit cell	Energy per adatom (reduced units $\times 10^2$)		Gap frequency (reduced units $\times 10^2$)	
	Hollow site	Bridge site	Hollow site	Bridge site
5	2.093 409	2.093 599	2.8990	unstable
7	1.997 087	1.997 058	unstable	1.5700
9	2.096 928	2.069 32	0.7768	unstable
11	2.217 134	2.217 133	unstable	0.3500
13	2.326 183	2.326 183	0.1405	unstable
15	2.419 627	2.419 627	unstable	0.0466

$\alpha=0.40$ all branches have optical character, with a very large gap even for the lowest case. As we have seen earlier, $\alpha=0.05$ is small enough that the cost in energy to slide the adsorbate line along the substrate is very small. By the time $\alpha=0.40$, the adsorbates are tightly locked onto the substrate, and the adsorbate/substrate complex is quite a rigid structure. Note that Fig. 3(c) shows, schematically, the relaxed equilibrium positions of the adsorbates.

For the one-dimensional line, for $\alpha=0.05, 0.10,$ and 0.40 , we have calculated room-temperature root-mean-square (rms) displacements in Table VI. These are based on $x_0=2.49 \text{ \AA}$, and the Ag-Ag force constant mentioned earlier. For $\alpha=0.05$ and 0.10 , the rms displacements are very large. These are so large, in fact, that harmonic lattice dynamics is of questionable accuracy. An increase of α from 0.10 to 0.40 reduces the calculated displacement dramatically, into the range where the harmonic approximation is surely reasonable. It should be remarked that a continued fraction technique has been used to calculate the mean-square displacement; we find this works very well.

In Fig. 4 we show information on the phonon spectrum

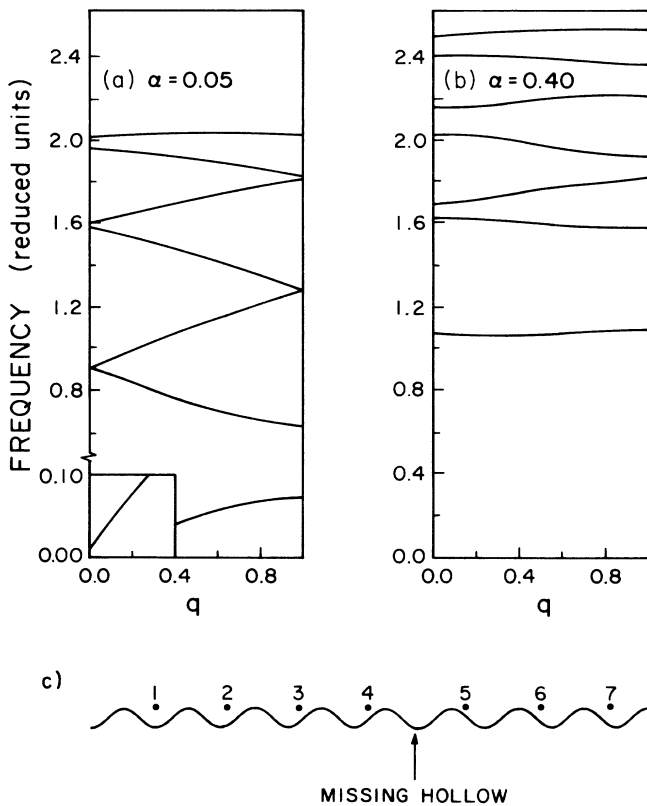


FIG. 3. Phonon dispersion curves for the one-dimensional case (a) for $\alpha=0.05$ and (b) for $\alpha=0.40$. In (a), the inset shows the lowest branch near $q=0$ on a scale expanded by a factor of 10 scale; so the gap in the phonon spectrum is evident. Reduced units of both frequency and wave vector are employed, and the Brillouin zone is that appropriate to a unit cell which contains seven atoms. In (c) we sketch the relaxed position of the adsorbates. Note that atom 1 is in a hollow site.

TABLE VI. Root-mean-square displacements (room temperature) for the one-dimensional adsorbate array, for various corrugation strengths [see Fig. 3(c)].

Atom no.	α (\AA)		
	0.05	0.10	0.40
1	0.63	0.17	0.07
2	0.75	0.22	0.07
3	1.04	0.38	0.07
4	1.38	0.66	0.10
5	1.38	0.66	0.10
6	1.04	0.38	0.07
7	0.75	0.22	0.07

on the two-dimensional overlayer, on the corrugated surface. The wave vector is directed parallel to the rows of atoms. The very first figure, Fig. 4(a), shows the phonon spectrum calculated in the absence of substrate corrugation. We have a perpendicularly polarized mode of Ein-

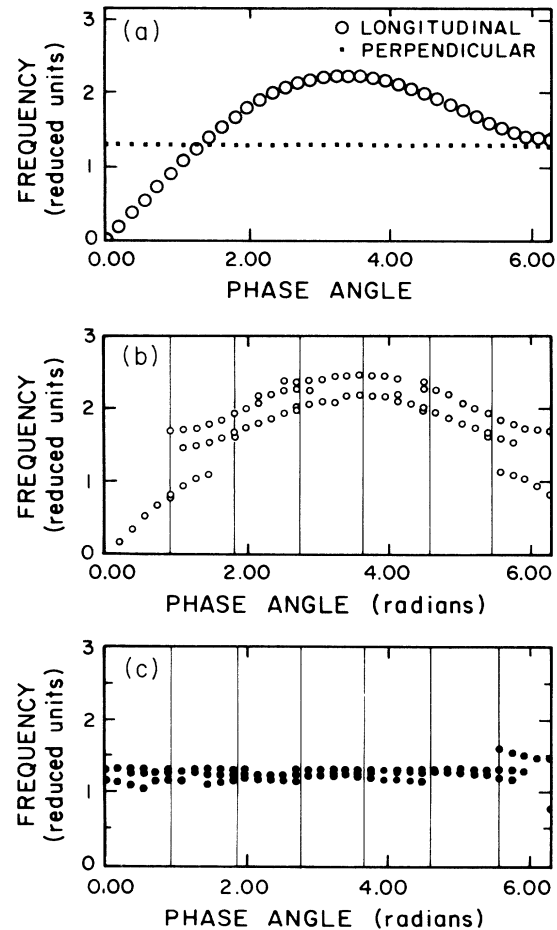


FIG. 4. (a) The dispersion relation of the longitudinal (open circles) and perpendicular mode (solid dots) of the two-dimensional adsorbate layer on a perfectly smooth surface. (b) Trajectories of the principal structures in the spectral density for longitudinal motion, for $\alpha=0.12$. (c) Trajectories of the principal structures in the spectral density for perpendicular motion for $\alpha=0.12$. In all cases, the Brillouin zone is that appropriate to the substrate, in the absence of the overlayer.

stein character. The frequencies of this mode are given as solid dots. We then have a purely longitudinal mode for the monolayer over the smooth substrate. As the wave vector approaches zero, this becomes a true acoustic mode, with linear slope and frequency that vanishes in the long-wavelength limit. It should be remarked that the Brillouin zone chosen in Fig. 4 is that appropriate for the substrate, in the absence of the overlayer.

Now, when corrugation is introduced, we may examine its influence by presenting information in the Brillouin zone used in Fig. (4a). Before we do this, we comment qualitatively on the influence of corrugation. First, of course, in the presence of corrugation induced "rumpling," the monolayer modes are neither purely perpendicular nor purely longitudinal, but have mixed character. We find these admixture effects are small throughout the zone. More importantly, the corrugation "mixes" modes with wave vector q with wave vectors $q+mG$, with G the reciprocal lattice vector associated with the minizones of the actual structure. Thus, if we plot the frequency spectrum associated with the wave vector q , we see several contributions. One is from the "direct" mode, which survives as the mode of wave vector q in the limit of vanishing corrugation (the presence of corrugation shifts its frequency, of course), and then we have contributions from the waves that are "direct" modes in the above sense of wave vector $q+mG$, which now contain admixtures of motions of wave vector q , by virtue of the corrugation induced mixing of eigenvectors.

In Figs. (4b) and (4c), for the longitudinal and perpendicular spectral densities, we plot the trajectories of the prominent features in the spectral densities, as a function of wave vector. The full spectral densities are rather complex, with rather substantial fine structure. We have isolated the prominent features by plotting only those points that corresponded to structures with peak intensity greater than a certain cutoff.

The principal effect of corrugation on the longitudinal spectral peaks is to produce doublets, at the large wave vectors. There is also clear evidence for "minigaps" at the various zone boundaries. As $q \rightarrow 0$, there is now a gap in the lowest frequency branch, but this is too small to be apparent in Fig. (4b).

In Fig. (4c) we have a similar plot for the perpendicular motion. The corrugation-induced alterations in the spectral plot are more modest than for the longitudinal modes. We again have a doublet structure, but these may be hard to resolve in an experiment that offers the resolution of the measurements in Ref. 5. Indeed, in these measurements, there is no evidence for such corrugation-induced structures in the spectral density, although the theory presented there does show that certain corrugation-induced-mode mixings play a vital role in the interpretation of the data.

In Table VII we show root-mean-square displacements for the various adsorbates, in the two-dimensional 2D overlayer, for $\alpha=0.12$. (To set the calculation up in 2D, as a simplification, the force from the substrate on each adsorbate perpendicular to the Ag rows was taken equal in magnitude to that experienced by a Ag atom in the hollow sites, parallel to the rows.) The shear horizontal

TABLE VII. Room-temperature root-mean-square displacements (in Å) for various atoms in the two-dimensional adsorbate overlayer, for the case where the corrugation parameter $\alpha=0.12$. The terms shear horizontal (SH) and longitudinal (L) refer to a direction parallel to the rows of adsorbate atoms, which is the y direction.

Atom		$\alpha=0.12$ Bridge symmetry
1	x (SH)	0.09
	y (L)	0.52 (bridge site)
	z (\perp)	0.13
2	x	0.09
	y	0.49
	z	0.21
3	x	0.10
	y	0.40
	z	0.22
4	x	0.10
	y	0.40 (near hollow)
	z	0.13

(reckoned relative to the direction of the adlayer rows) and perpendicular displacements are modest in magnitude and typical of those calculated for atoms in various crystal surfaces. The longitudinal motions are very large and, in fact, sufficiently large to call the results generated by the harmonic approximation into question. This system should be explored within the framework of molecular dynamics before quantitative conclusions can be reached. We have such studies underway. It is clear, however, that root-mean-square displacements parallel to the surface are very large, for the reasons outlined earlier in this paper.

IV. CONCLUDING REMARKS

We have investigated the energetics and lattice dynamics of adlayers we refer to as nearly incommensurate, a term defined in Sec. I. For modestly corrugated surfaces, the discussion in Sec. II, and numerical calculations presented subsequently show that the "lock-in" energy is remarkably small. When the lattice vibrations of such an overlayer are analyzed in the rigid substrate approximation, we find a very small gap in the lowest branch of the phonon spectrums. This has the consequence that in the harmonic approximation, the longitudinal mean-square displacement is very large indeed.

As our corrugation strength parameter α is increased, we find that the lock-in energy begins to increase rapidly. The system stiffens up, and the longitudinal component of mean-square displacement becomes rather ordinary in magnitude. The transition between these two regimes is gradual; i.e., when we vary the corrugation parameter α , all properties we examine in our mean-field description vary continuously with α .

The transition between the weakly and strongly locked regimes occurs when $\alpha \cong 0.20$. Application of our model

to the Ag overlayer on Ni(100) suggests that for this system, $\alpha=0.12$. We are in the regime where we expect the mean-square displacement parallel to the surface to be large, but close to the crossover to strongly locked in behavior. We may expect the nearly incommensurate metal overlayers on metal substrates will exhibit both behaviors, since rather modest changes in model parameters will take us from one regime to the other.

Our results for the mean-square displacement suggest that molecular dynamics should be used to study the atomic motions in such systems. Also, it would be of

great interest to incorporate substrate atom motions into the analysis. We have new studies underway with these goals in mind.

ACKNOWLEDGMENTS

The research of one of us (D.L.M.) was supported by Grant No. 20572-AC5 of the Petroleum Research Fund of the American Chemical Society. The research of the other (J.E.B.) was supported by the Natural Sciences and Engineering Research Council of Canada.

¹K. D. Gibson, S. J. Sibener, Burl M. Hall, J. E. Black, and D. L. Mills, *J. Chem. Phys.* **83**, 4256 (1983).

²See K. Kern and G. Comsa, in *Chemistry and Physics of Solid Surfaces VII*, edited by R. Vanselow and R. Howe (Springer, Heidelberg, 1988), p. 65.

³In an overlayer on a crystal, it is possible for the structure to be incommensurate as one moves in one direction, say, along the x direction, but commensurate along a second noncolinear

direction.

⁴R. F. Wallis, *Prog. Surf. Sci.* **4**, 233 (1973).

⁵W. Daum, C. Stuhlman, H. Ibach, J. E. Black, and D. L. Mills, *Surf. Sci.* **217**, 529 (1989).

⁶P. Bak, *Rep. Prog. Phys.* **45**, 587 (1987).

⁷J. E. Black, F. Shanes, and R. F. Wallis, *Surf. Sci.* **133**, 199 (1983).